Modulation of Localized Surface Plasmon Resonance of Nanostructured Gold Crystals by Tuning Their Tip Curvature with Assistance of Iodide and Silver(I) Ions

ARTICLE *in* THE JOURNAL OF PHYSICAL CHEMISTRY C · AUGUST 2011

Impact Factor: 4.77 · DOI: 10.1021/jp111605j

3 AUTHORS, INCLUDING:

Zhengbo Jiao
Chinese Academy of Sciences
30 PUBLICATIONS **489** CITATIONS
SEE PROFILE

Haibing Xia
Shandong University
45 PUBLICATIONS **840** CITATIONS
SEE PROFILE

THE JOURNAL OF PHYSICAL CHEMISTRY C

ARTICLE

pubs.acs.org/JPCC

Modulation of Localized Surface Plasmon Resonance of Nanostructured Gold Crystals by Tuning Their Tip Curvature with Assistance of Iodide and Silver(I) Ions

Zhengbo Jiao, Haibing Xia,* and Xutang Tao*

State Key Laboratory of Crystal Materials, Shandong University, Jinan, 250100, P. R. China

Supporting Information

ABSTRACT: In this article, we describe a series of experiments that systematically addressed and clarified the effects of iodide, silver ions, and ascorbic acid (AA) concentration on the morphology of gold nanorods (Au NRs) during the overgrowth process. When iodide ions, silver ions, or both were present in the growth solution, a morphology of Au nanocrystals ranging from thick NRs, cuboidal shaped NRs, dogbone-like NRs, to dumbbell NRs, respectively, was obtained. The appearance of the third peak in the UV−vis spectra indicates the formation of lobes on the tips of Au NRs. In addition, when different seeds (such as Au NRs of short aspect ratio and spherical Au nanocrystals) whose {111} facets were covered by iodide ions were used, horns of different length on Au seeds were formed. Taken together, the results mentioned above and cross section change of the tips of Au NRs, two lobes instead of four formed on each tip of the Au NRs are explained for the first time, and their growth from {111} facets is assisted by the formation of AgI, which can catalytically reduce Au ions into atoms on those facets. The optical spectra of nanostructured Au crystals can be tuned from 520 to 955 nm by controlling their tip curvature or platinum coating. A wide color gamut can be readily obtained by using a random dispersion of nanostructured Au NR-based crystals.

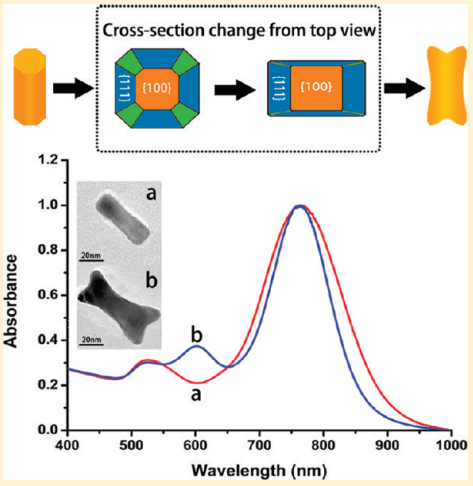

1. INTRODUCTION

Colloidal growth of nanocrystals (NCs) has been widely studied in nanoscience and nanotechnology in the past few years. It is one effective way to control the size and morphology of NCs, which are crucial to their properties.[1,2] Plasmonic optical response of noble metal NCs has been widely studied over the past decades, and it is related to localized surface plasmon resonance (SPR) from visible to near-infrared range.[3−10] Especially, nanostructured Au crystals have aroused more interest than the others[11] because of their unique size-dependent color and tuned SPR in a wide spectral range by simply controlling their aspect ratio. Currently, it is well-known that the frequency of SPR is dependent mainly on the size, shape, and composition of nanoparticles as well as the dielectric properties of the surrounding medium.[12−17] Au nanocrystals of simple geometries, such as sphere,[18,19] rod,[20−25] cube,[26−28] and triangular prism[29,30] have been successfully synthesized with excellent control of quality and yield. However, the overgrowth of preformed NCs has been less studied, although it could offer novel synthetic control for their morphology. Recently, rhombic dodecahedron and concave nanocubes with high-energy facets, such as {110} and {720}, have also been exploited, which would be rather useful in optical and catalytic applications.[31,32] Therefore, it is desirable to intentionally control the growth process to achieve the programmed shape control of NCs to finely control their properties.

Among nanostructured gold of different shapes, nanorods are still considered as a rather useful and flexible morphology, mainly because of their optical spectra sensitivity to changes of shape and volume and the recent experimental breakthroughs in the preparation of short aspect ratio single crystalline gold nanorods (Au NRs) with a good reproducibility and high yield.[20−25] Au NRs have two surface plasmon resonance absorption modes associated with the oscillation of conduction electrons. The transverse surface plasmon is not influenced much by the aspect ratio[33] of Au NRs, but longitudinal surface plasmons (LSPs) are sensitive to the aspect ratio[20] and can be tuned easily from visible to near-infrared by precisely controlling their size, shape, and environment. The optical properties of nanostructured gold crystals mentioned above render them ideal candidates for a large number of applications, such as optical addressable diagnostic methods, therapies, optical data storage,[34] and surface enhanced Raman spectroscopy.[35,36] Therefore, controlling the morphology of nanostructured Au crystals is also technologically important.[37]

Recently, the influence of halide ions on the morphology of Au NRs has been investigated widely. For example, Ha et al. reported

Received: December 6, 2010
Revised: March 21, 2011
Published: March 31, 2011

that three different morphologies of Au crystals were prepared by solely controlling the amount of halide ions in the growth solution.[29] Mirkin's group also reported that one reaction can be driven to predominantly produce one of the three target morphologies (rods, prisms and spheres) by adjusting iodide concentration.[38] Liz-Marzán and co-workers found that the tip growth of Au NRs can be greatly enhanced in the presence of a tiny amount of iodide and resulted in the formation of a well-defined dumbbell morphology.[39] In addition, silver ions also play a crucial role in the formation of nanostructured Au crystals and control of their morphology. Song et al. successfully produced a series of Au NCs in the shape of octahedrons, truncated octahedrons, cub-octahedrons, cubes, and higher polygons by incremental changes of silver nitrate concentration in the modified polyol process.[28] Xiang et al. successfully obtained the arrow-headed Au NRs and gold nano-octahedron by introducing silver ions that switched the growth mode of Au NRs from {110} restriction to preference.[3]

The role of halide and silver ions in the formation and growth of gold NCs has been widely discussed.[38−44] It is well-known that halide ions can adsorb on gold surfaces and that their binding energies scale with polarizability ($I^- > Br^- > Cl^-$) and crystal facets ((111) > (110) > (100)).[38,40] The underpotential deposition (UPD) shifts of silver over gold surfaces are in the order of (110) > (100) > (111).[44] It was suggested in previous studies that the growth rate of the facets of Au NR adsorbed halide or silver ions would be significantly influenced.[38,44] For instance, dumbbell-like Au NCs were prepared in the presence of a tiny amount of iodide in the growth solution.[39] Dogbone-like (two lobes on each tip) Au NCs were produced by further adding ascorbic acid into the growth solution of Au NRs after the reaction termination[25] or by aging Au NRs over a certain time.[33] However, the actual influence factors that induce the formation of a dogbone-like structure have not been confirmed: for example, why two lobes instead of four are formed on each tip of the Au crystals because the four {111} facets on each tip of the Au NRs are equivalent. In addition, it was occasionally found that optical properties of Au NRs were able to be affected obviously by a small change at the tips. Furthermore, the Cortie group reported that in their simulation results, there should be the appearance of a third peak around 560 nm in the optical extinction spectrum. However, to the best of our knowledge, three obvious peaks in the UV−vis spectra of dogbone-like Au NCs were rarely observed. On the basis of previous studies, it is possible that the UV−vis spectra cannot correspond to the final Au products, considering the instability of Au NRs in the solution.

In this article, we describe a series of experiments that systematically addressed and clarified the effects of iodide, silver ions and AA concentration on the morphology of Au NRs as seeds during the overgrowth process. When iodide ions, silver ions, or both were in the growth solution, the morphology of the Au NCs ranging from thick NRs, cuboidal shaped NRs, and dogbone-like NRs to dumbbell NRs was obtained. The appearance of the third peak in the UV−vis spectra indicates the formation of lobes on the tips of Au NRs. In addition, when different seeds (such as Au NRs of short aspect ratio and spherical Au NCs) whose {111} facets were covered by iodide ions were used, horns of different length on Au seeds were formed. Taken together, the results mentioned above and cross section change of the tips of the Au NRs and why two lobes instead of four are formed on each tip of the Au NRs is explained for the first time, and their growth from {111} facets is assisted by the formation of AgI, which can catalytically reduce Au ions on those facets. The optical spectra of nanostructured Au crystals can be tuned from 520 to 955 nm by controlling their tip curvature or platinum coating. A wide color gamut can be readily obtained by using a random dispersion of nanostructured Au NR-based crystals.

2. EXPERIMENTAL SECTION

2.1. Chemicals. Cetyltrimethylammonium bromide (CTAB) (99%) was purchased from Sigma-Aldrich. $HAuCl_4 \cdot 3H_2O$ (99.9%) and $AgNO_3$ (99+%) were obtained from Alfa. $NaBH_4$ (99%) and AA (99+%) were purchased from Sinopharm Chemical Reagent Co., Ltd. Milli-Q water (18 MΩ cm, Millipore) was used for all solution preparations. Glassware was cleaned by soaking in aqua regia and finally washing with Milli-Q water.

2.2. Preparation of Gold Seeds. Gold seeds were synthesized by the method described by Nikoobakht et al. with minor modification.[23] In general, 250 μL of 10 mM $HAuCl_4$ was added to 7.5 mL of 0.1 M CTAB solution. Next, 0.6 mL of freshly prepared 10 mM $NaBH_4$ was added to the solution with vigorous stirring. The color of the solution changed from yellow to brown. The solution was vigorously stirred for 2 min and then kept at room temperature for 3 h to ensure full decomposition of excess $NaBH_4$.

2.3. Synthesis of Gold Nanorods. The gold nanorods were prepared by the seed-mediated, surfactant-directed growth method.[21,23] The growth solution of gold nanorods consisted of 5 mL of 0.1 M CTAB, 200 μL of 10 mM $HAuCl_4$, and 30 μL of 10 mM $AgNO_3$; 32 μL of 0.1 M AA was then added. After the color of the solution changed from orange to colorless, 10 μL of the seed solution was added to the growth solution under stirring for about 20 s. The resulting mixture was left undisturbed and aged for 3 h at room temperature before use.

Different aspect ratios of Au NRs were prepared by adding different amounts of KI to the growth solution. Five milliliters of 0.1 M CTAB was first mixed with different amounts of KI. $HAuCl_4$ (200 μL, 10 mM), $AgNO_3$ (30 μL, 10 mM), and ascorbic acid (32 μL, 0.1 M) were added in sequence. The concentrations of KI in the growth solution were 0.0005, 0.0013, 0.002, and 0.02 mM, respectively. After the color of the solution changed from orange to colorless, 10 μL of the seed solution was added to the growth solution under stirring for about 20 s. The resulting mixture was left undisturbed and aged for 3 h at room temperature before use.

2.4. Synthesis of Dogbone-Like and Dumbbell-Like Gold Nanoparticles. To investigate the influence of silver ions on gold nanorods without addition of iodide ions, a series of growth solutions were prepared, including CTAB (5 mL, 0.1 M) and $HAuCl_4$ (200 μL, 10 mM). The concentrations of additional $AgNO_3$ were 0, 0.04, 0.06, and 0.24 mM, respectively. Ascorbic acid (32 μL, 0.1 M) and gold nanorods (1 mL) were then added under stirring.

For the growth of gold nanorods in the presence of iodide ions and silver ions simultaneously, 5 mL of 0.1 M CTAB was mixed with different amounts of KI, followed by addition of $HAuCl_4$ (200 μL, 10 mM), $AgNO_3$ (30 μL, 10 mM), and ascorbic acid (32 μL, 0.1 M). The concentration of KI ranged from 0.001, 0.004, 0.008, 0.016, and 0.04 to 0.16 mM, respectively. Finally, a gold nanorod seed solution (1 mL) was added under stirring.

While maintaining the concentration of KI (0.5 μL, 10 mM) but varying the amounts of $AgNO_3$, the same procedure mentioned above was followed. The concentration of $AgNO_3$ ranged from 0, 0.01, 0.04, and 0.08 to 0.16 mM, respectively.

Scheme 1. Schematic Illustration of the Influence of Iodide Ions or Silver Ions or Both on the Morphology of the Au NRs during the Growth Process[a]

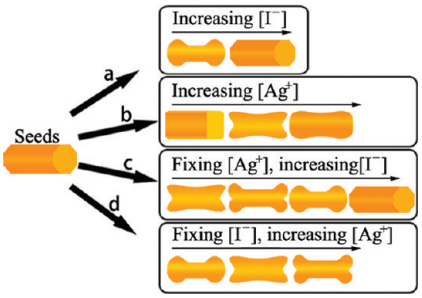

[a] (a) Morphology change of Au NRs from rod, dumbbell, to thicker rod with increasing concentration of iodide ions. (b) Morphology change of Au NRs from rod, cuboid, dogbone-like with sharp lobes to "I"-shape with increasing concentration of silver ion. (c) Morphology change of Au NRs from rod, dogbone-like with sharp lobes, dogbone-like with obtuse lobes, dumbbell to thicker rod with increasing concentration of iodide ions at fixed concentration of silver ions. (d) Morphology change of Au NRs from rod, dumbbell, dogbone-like with sharp lobes to dogbone-like with increasing concentration of silver ions at fixed concentration of iodide ions.

When different aspect ratios of Au NRs were used as seeds, the growth solution of gold nanorods consisted of 5 mL of 0.1 M CTAB, 200 μL of 10 mM $HAuCl_4$, and 30 μL of 10 mM $AgNO_3$; 32 μL of 0.1 M AA was then added. After the color of the solution changed from orange to colorless, 1 mM of as-prepared Au NCs seeds with different aspect ratios was added then under stirring.

2.5. Synthesis of $Au_{core}Pt_{shell}$ NRs. Five milliliters of 0.1 M CTAB was mixed with different amounts of K_2PtCl_4, followed by addition of $AgNO_3$ (30 μL, 10 mM) and ascorbic acid (32 μL, 0.1 M). The concentration of K_2PtCl_4 ranged from 0.05, 0.125, 0.2, and 0.275 to 0.35 mM, respectively. Finally, a gold nanorod seed solution (1 mL) was added under stirring.

2.6. Instruments. Scanning electron microscopy (SEM, Hitachi S-4800) was used to determine the shape and size of the nanorods. Optical characterization was carried out by UV−vis spectroscopy with a Cary 50 spectrophotometer, using 10 mm path length quartz cuvettes. Transmission electron microscopy (TEM) images were obtained with a JEOL JEM 1011 transmission electron microscope operating at an acceleration voltage of 100 kV, and the high-resolution TEM (HRTEM) images were obtained using a Philips Tecnai 20U-TWIN microscope operating at 200 kV.

3. RESULTS AND DISCUSSION

3.1. Preparation of Au NR Seed. The effect of iodide, silver, or both on morphology changes of the Au NRs in the growth solution was investigated in this work (Scheme 1). The seeds of Au NRs were prepared by the well-known "seed-mediated" growth method with minor modifications.[23,44,45] The aspect ratio of as-prepared Au NRs was ~3, as shown in Figure 1a. Other aspect ratio of Au NRs and spherical NCs were prepared by adding a proper amount of iodide ions in the growth solution. These seeds of Au NRs were purified by centrifugation to remove remaining reactants and byproducts before use. The corresponding amount of CTAB solution was supplemented to keep the Au NRs at their original concentration. One milliliter of Au NR seed

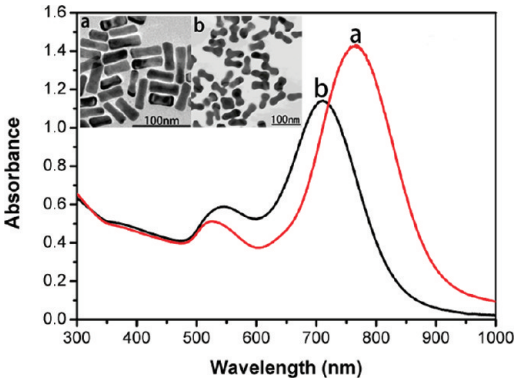

Figure 1. (a) UV−vis spectra of as-prepared seeds of Au NRs and (b) dumbbell-like Au NCs prepared by addition of proper amount of iodide ions in the growth solution. The insets are their TEM images.

solution was used in all the experiments except as noted specifically. The concentration of CTAB, $HAuCl_4$, Au NR seed, and AA in the growth solution was fixed. The morphology change of the Au NRs, especially at the tips, was tuned by addition of silver ions, iodide ions, or both.

3.2. Influence of Iodide Ions Alone on Morphology of Au NRs. In a previous work by Liz-Marzán's group,[39] the effect of iodide on hte shape change of Au NRs in the growth solution was investigated in detail without addition of silver ions. The morphology of nanostructured Au crystals ranged from thick nanorods to dumbbell-like crystal (Figure 1b, Scheme 1a). It was proposed that it is likely related to the preferential adsorption of iodide ions on {111} faces, as compared with {110} and {100}. Subsequently, gold ions were catalytically reduced on the {111} surfaces coated by AgI, where the surface redox potential is lower, leading to dumbbell formation.

In our case, the effect of silver ions (Scheme 1b), the effect of iodide in the presence of silver ions (Scheme 1c), and the effect of silver ions in the presence of iodide ions (Scheme 1d) were investigated.

3.3. Influence of Silver Ions Alone on Morphology of Au NRs. In the control experiment, there were no silver ions or iodide ions in the growth solution. The morphology of the as-prepared Au NRs was kept unchanged, and the aspect ratio was decreased to ~2 (Table 1). This indicates the preferential growth in the transverse direction other than in the longitudinal direction during overgrowth.

To investigate the influence of silver ions on the morphology of the Au NRs in the growth solution without any addition of iodide ions, a series of experiments were conducted by varying the amount of silver ions (see Figure 2 and Figure 3). When the concentration of silver ions in the growth solution was less than 0.06 mM, the cuboidal shaped Au NRs were obtained (Figure 3a and 3b), and the aspect ratio was also decreased to about 2. As such, at a fixed reaction condition, except for the concentration of silver ions, the finally increased volume of the Au substance on the Au NRs should be the same. The increase in the length and width at the same aspect ratio indicated that their height became smaller when silver was increased from 0 to 0.04 mM. Some Au NRs were upstanding, and their tips can be visualized. The SEM images are shown in Figure 4a and b. Their atomic force microscopy (AFM) images and large-area SEM images are shown in Figures S1 and S2, respectively, of the Supporting Information. As expected, the tip of the Au NRs from a top view

Table 1. Average Values of L, D_1, D_2, L/D_1, and L/D_2 for Au NR Seeds and Final Au NR-Based NCs Prepared by Addition of Different Amounts of Silver Ions [a]

sample	$AgNO_3$ (mM)	L (nm)	D_1 (nm)	D_2 (nm)	L/D_1	L/D_2
Au NRs		47.41 ± 6.2	16.15 ± 3.6	16.15 ± 3.6	2.94 ± 0.33	2.94 ± 0.33
a	0	60.66 ± 9.3	30.11 ± 4.4	30.11 ± 4.4	2.01 ± 0.71	2.01 ± 0.71
b	0.04	68.62 ± 9.2	34.16 ± 7.1	34.16 ± 7.1	2.01 ± 0.79	2.01 ± 0.79
c	0.06	72.34 ± 8.5	31.25 ± 6.5	35.85 ± 5.2	2.31 ± 0.82	2.02 ± 0.63
d	0.24	67.81 ± 8.8	28.91 ± 6.8	31.02 ± 6.3	2.34 ± 0.76	2.19 ± 0.65

[a] The range given is the standard deviation of the measurement. L is the length, D_1 is the diameter of the mid section, D_2 is the maximum diameter of the ends, and the L/D_1 or L/D_2 is the aspect ratio.

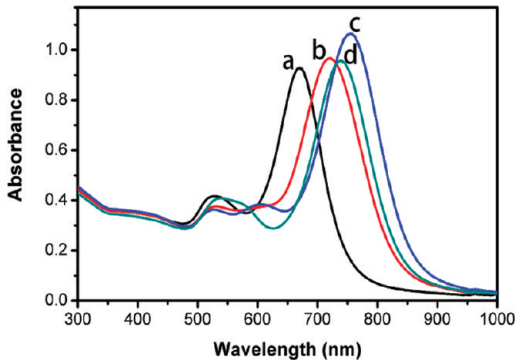

Figure 2. UV−vis spectra of the resulting Au NCs produced in the presence of different concentrations of silver ions without addition of iodide ions. The final concentrations of silver ions in the growth solution are (a) 0, (b) 0.04, (c) 0.06, and 0.24 mM, respectively.

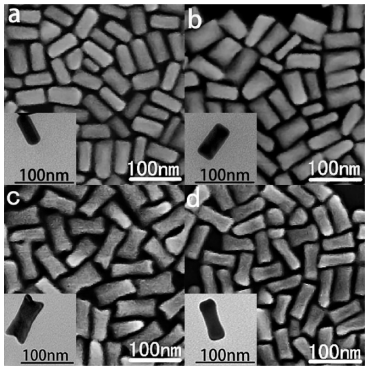

Figure 3. SEM images of the resulting Au NCs produced in the presence of different concentrations of silver ions without addition of iodide ions. The final concentrations of silver ions in the growth solution are (a) 0, (b) 0.04, (c) 0.06, and (d) 0.24 mM, respectively.

changed from cuboctahedron (about 30 nm × 30 nm) to truncated rectangular−octahedron (about 35 nm × 20 nm). Therefore, the area of the original facets (about 15 nm × 15 nm) on the tips should be affected during growth in the presence of a high concentration of silver ions.

The crystal structure of Au NRs has been investigated by Wang et al. using high-resolution TEM. It was found that the side facets of the Au NRs were dominated by four {110} and four {100} facets, whereas the ends of the NRs were enclosed by {111} and {110} facets of small area.[46] In addition to those prepared by electrochemical methods, the Au NRs synthesized by the Ag(I)-assisted seed-mediated technique also have the

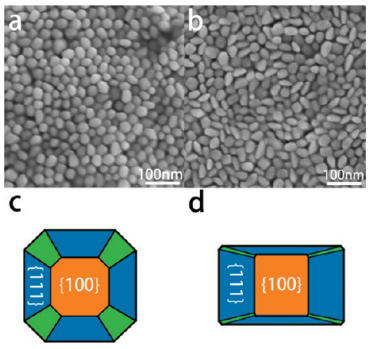

Figure 4. SEM images from a top view of as-prepared Au NCs produced (a) in the absence of silver ions and (b) in the presence of silver ions (0.04 mM). (c, d) Schematic illustration of a top view of as-prepared Au NCs a and b, respectively.

same crystal structure.[34,44,46,47] According to the underpotential deposition theory, a metal submonolayer or monolayer can be deposited onto a different metal surface at a potential significantly less negative than for bulk deposition.[48] Thus, a silver monolayer on Au NRs may be expected, and the UPD shifts of silver on gold surfaces are in the order of (110) > (100) > (111).[44] The growth rate of the gold facets with a silver monolayer may be significantly slowed down. During the formation of Au NRs, silver atoms selectively adsorb onto Au {110} facets according to the UPD theory, which restricts the deposition of Au atoms on them and induces the deposition on {100} and {111} surfaces, thus leading to the growth of Au NRs along the [100] direction.[44]

Considering their rectangular cross section and high probability to be imaged, we suggest that the {110} side facets might be dominant side facets for final Au NRs. The four {110} side facets grow more slowly than the four {100} side facets due to strong stabilization of CTAB and the silver layer on the {110} facets to inhibit their growth. In addition, among the four {110} facets, the growth rates are also different. One pair of opposite {110} side facets grow more quickly than another pair, thus resulting in a truncated rectangular cross section (Figure 4b). A similar phenomenon was observed in Xiang's work, and one assumption was proposed that the sizes of the four {110} side facets are different, which thus leads to their different growth rate. It was known that silver ions played a key role in the synthesis of Au NRs. It was proposed that AgBr formed at gold−CTAB interfaces would deposit on Au rod surfaces to direct growth by hindering growth from a specific facet, thus promoting growth on the less densely covered facets.[49,50] Furthermore, it was also reported by Huang[51] that the isotropic and anisotropic growth of

Au NRs during the overgrowth process were affected by the concentration of CTAB. Similarly, in the overgrowth of Au NRs, the silver monolayer formed acts as a strongly binding surfactant to protect the facets of Au NRs from further growth.[44] Therefore, different growth rates of {110} facets also can be induced by different coverage of silver ions due to their different concentrations.

In our case, at a low concentration of silver ions, it is possible that silver ions were not enough to cover all the four {110} side facets gradually as these areas of {110} side facets were increased during growth. Subsequently, the growth rate of the {110} side facets would be different due to different coverages of the silver layer. Accordingly, the cross section of the final Au crystals becomes rectangular. During the growth of Au NRs, it is the equilibrium of competition between minimization of the surface energy and strong stabilization of the CTAB surfactant on {110} facets. The fast growth of four {100} side facets would limit growth of the connected {110} facets at the tips. This is energetically beneficial.

Meanwhile, the slow growth of four {110} side facets would lead to enlargement of the connected {111} facets at the tips. This is also energetically beneficial. Due to the different growth rates of the four {110} side facets, the four {111} facets at the tips were also different (Figure 4c and d). Hence, this growth model would induce a decrease in the overall surface energy of the Au NCs and is reasonable. Finally, two lobes instead of four protruded from two bigger {111} facets of each tip and further evolved into dogbone-like Au crystals during growth of the Au NRs when silver ions were changed.

When the concentration of silver ions in the growth solution was increased to 0.06 mM, Au NCs with dogbone-like structure were formed, as shown in Figure 3c. Surprisingly, a new peak centered at around 590 nm (the third peak) appeared in the UV−vis spectrum. In addition, a maximum development of the LSP peak around 755 nm was achieved. The third peak was gradually developed, and the LSP peak was red-shifted from 670 to 755 nm (Figure 2a−c) when the concentration of silver ions was increased from 0 to 0.06 mM. However, when the concentration of silver ions was >0.06 mM, the two lobes of the dogbone-like gold NCs started to merge into "I"-shaped Au NCs (Figure 3d). Accordingly, the third peak gradually merged into the first peak centered at about 520 nm and the LSP peak was then blue-shifted to 737 nm (see Figure S3 for all of the UV−vis spectra recorded under different concentrations of silver ions). The results are in agreement with the simulation result conducted by Cortie's group.[33]

The bulk deposition of silver on the surface of gold nanorods by reduction of ascorbic acid in the current growth solution could not happen because the current pH is about 3.[44,49,50] As expected, there is no characteristic silver plasmon band at ~400 nm in the UV−visible spectra.[43,44] Therefore, the two lobes on Au NRs were not formed by silver. Obviously, the presence of silver ions during the growth of Au NRs causes the morphology to change from cylindrical to dogbone structure. According to the simulation results, the development of dogbone-like shapes leads to a red shift of the LSP band and the development of the third peak, which is caused by the loss of rotation symmetry.[33] In addition, the position of the longitudinal plasmon is more strongly influenced by the ratio of L/D_1 rather than L/D_2, which was also in agreement with our results (Table 1).

According to the correlation between the aspect ratio and the peak position of the plasmon band, the observed shifts indicate an increase in the aspect ratio for a low concentration of silver ions and a decrease for a high one. However, the SEM results were in conflict with these predictions. All four Au NRs should have the same volume because the same amount of Au NR seeds was grown in the same amount of growth solutions except for the tiny amount of silver ions, which could not be reduced. Although the aspect ratio of sample a and sample b is the same, the LSP of sample b was red-shifted due to their shape became cuboid, not cuboctahedron. The cross section of their tip also changed from cuboctahedron to rectangular (Figure 4a and b). This red shift of nanostructured Au crystals at the same aspect ratio and volume (Figure 2a to c) was attributed to their shape, which has an effect on the extinction spectra. The position of the LSP band of sample c was bigger than that of sample d due to the dogbone-like shape, despite the aspect ratio of sample c being smaller than sample d.

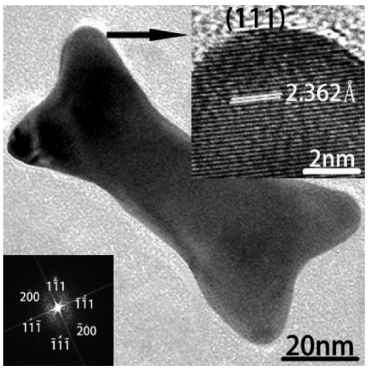

Figure 5. High-resolution TEM image of a dogbone-like Au NC prepared in the presence of silver ions (0.06 mM) without the addition of iodide ions. The inset is the corresponding FFT image.

The HRTEM image of a dogbone-like Au crystal is shown in Figure 5. It was observed that the lobes of dogbone-like Au crystals grow along the [111] direction. Thus far, the roles of silver ions in regulating the shape of nanostructured Au crystals are not completely understood; however, on the basis of the above analysis and widely accepted UDP theory, it is reasonable that silver ions might preferentially adsorb on some of the {110} side facets and induce the anisotropic growth of preformed Au NRs used as seeds. When the concentration of silver ions was below 0.06 mM, the cuboid structure with less thickness was formed. The dogbone-like structure was obtained when the concentration of the silver ions was 0.06 mM.

The possible surface area and arrangement of all facets at the tips of the cuboid Au NRs are shown in Figure 4c and d. It was assumed that the amount of silver ions (0.06 mM) may be enough to form a silver monolayer on both the {110} and {100} facets on the tips. Because the growth rate of the two facets was firmly restricted but the remaining larger {111} facets on the tips were not covered by a silver layer and could grow randomly, the two protruding dog-bone lobes were then formed. Upon further increasing the amount of silver ions, the {111} facets at the tips could also be covered with a silver layer from partially to fully, with the two lobes of the dog-bone changing from protruding to obtuse and further merging together.

3.4. Influence of Iodide Ions on Morphology of Au NRs at Fixed Concentration of Silver Ions. It was reported that addition of proper amounts of iodide to the growth solution results in the growth of Au crystals with dumbbell-like structure.[39] It was found by us that the addition of appropriate amounts of silver ions leads to the formation of dogbone-like Au crystals. The two different morphologies have distinct UV−vis spectra, which could be readily tuned by a slight morphology

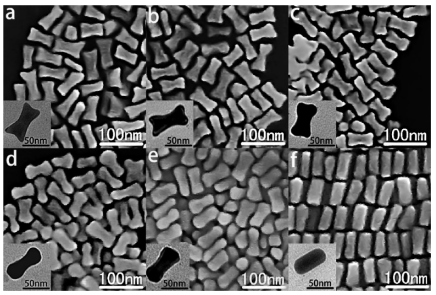

Figure 6. SEM images of Au NCs produced in the presence of different concentrations of iodide ions and at a fixed concentration of silver ions (0.06 mM). The final concentrations of iodide ions in the growth solution were (a) 0.001, (b) 0.004, (c) 0.008, (d) 0.016, (e) 0.04, and (f) 0.16 mM, respectively. The insets are their TEM images.

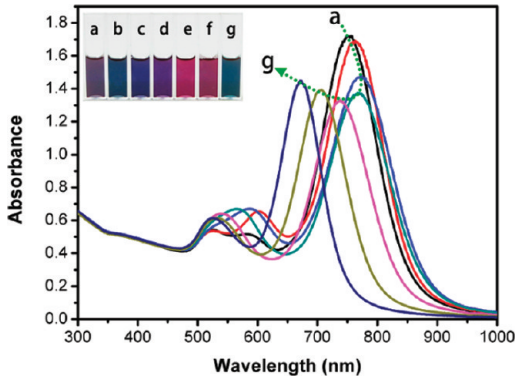

Figure 7. UV−vis spectra of Au NCs produced in the presence of different concentrations of iodide ions and at a fixed concentration of silver ions (0.06 mM). The final concentrations of iodide ions in the growth solution were (a) 0, (b) 0.001, (c) 0.004, (d) 0.008, (e) 0.016, (f) 0.04, and (g) 0.16 mM, respectively.

change of nanostructured Au NR-based crystals. Therefore, a wide color gamut can be readily obtained by using a random dispersion of nanostructured Au NR-based crystals.

To fabricate Au NR-based crystals with different morphology, the amount of additional iodide ions was varied at the fixed concentration of silver ions. The SEM images of the corresponding final nanostructured Au NR-based crystals are shown in Figure 6. Compared with previous nanostructured Au NR-based crystals prepared in the presence of silver ions alone, the presence of tiny amounts of iodide ions (0.001 mM) render the two lobes at the tips of dogbone-like Au crystals larger and more protruding. Gradually, the two lobes at the tips were changed from sharp (Figure 6a) to obtuse (Figure 6b and c) and merged together to form the dumbbell (Figure 6d and e) when the concentration of iodide ions was increased (see Table S1 for more details).

In addition, the length of the lobes and the diameter of the middle part were decreased and increased gradually, respectively. Eventually, the morphology of the Au NRs remained cylinder-shaped, and their size in length and width became bigger (Figure 6f) when the concentration of iodide ions reached 0.16 mM. Accordingly, the intensity of the third peak of nanostructured Au crystals around 590 nm in the UV−vis spectra (shown in Figure 7) was greatly enhanced (Figure 7b) in the presence of tiny amounts of iodide ions (0.001 mM). While increasing the amounts of iodide ions in the growth solution, the third peak was gradually blue-shifted and merged into the first peak (Figure 7c−g). The position of the LSP band was slightly red-shifted from 753 to 773 nm (Figure 7a−c) when the concentration of iodide ions was increased from 0.001 to 0.008 mM. Subsequently, it was gradually blue-shifted from 768 to 670 nm due to the decrease in the aspect ratio of L/D_1.

The morphology transition from dogbone, dumbbell to rod finally was readily achieved by adjusting the concentration of iodide ions at a fixed concentration of silver ions. It was known that halide ions adsorb on gold surfaces in the order of (111) > (110) > (100), and the growth rate of the facets covered by iodide ions could be greatly enhanced.[39] When a small amount of iodide ions (0.001 mM) was used, only the {111} facets at the tips were selectively covered, leading to the formation of AgI, followed by reduction of the gold salt precursor due to a decrease in the surface redox potential. As a result, the lobes of dogbone-like Au crystals grew larger. Accordingly, the intensity of the third peak in UV−vis spectra was enhanced. With an increase in the concentration of iodide ions, the growth rate of other facets on the tips was also increased gradually due to the coverage of iodide ions on them. Therefore, the lobes of dogbone-like Au crystals joined together gradually and developed into dumbbell-like crystals eventually. When the concentration of iodide ions reached 0.16 mM, all the facets, including side facets, were covered by iodide ions. Subsequently, homogeneous growth leads to the formation of thicker Au NRs with a normal shape.

The requirement for the formation of dogbone-like Au crystals in the presence of silver ions or both silver and iodide ions was consistent with those for the formation of branched structures in the case of a semiconductor system.[52−55] The requirements are as follows:[56] (i) there is a relatively high supply of growth units to the seeds and (ii) the evolution of branches is determined by a competition balancing between the concentration buildup of the growth unit and ligand/stabilizing molecules on the facets.

In our case, the absorption of CTAB on {111} facets on the tips is the weakest among the facets of {111}, {100}, and {110}. In addition, the adsorption capability of the silver ions is in the order (110) > (100) > (111). Therefore, {111} facets are less stabilized by CTAB and easily grown. Furthermore, the additional iodide ions absorbed on {111} facets to form AgI with silver ions. The formation of AgI would lead to the growth unit of Au atoms concentrated in the vicinity of the {111} facets because AgI can catalytically reduce gold ions into gold atoms. Subsequently, the lobes on the tips of Au NRs were grown from {111} facets. Due to the interesting results mentioned above, the effect of silver ions on the morphology of Au NRs at a fixed concentration of iodide ions was also conducted. In addition, it will be useful to tell the role of silver and iodide ions in the morphology change.

3.5. Influence of Silver Ions on Morphology of Au NRs at a Fixed Concentration of Iodide Ions. The morphology of all the resulting dogbone-like Au crystals (see Figure S4) is the same, except that the length of the lobe on the tips when the concentration of silver ions was varied under a fixed concentration of iodide ions (see Table S2 for detailed information). The length of the lobe on the tips is ~13.5, 14.5, and 12.1 nm for samples b, c, and d, respectively. Although there is a minor difference in length, there is a remarkable difference in their UV−vis spectra (see Figure S5 for all the UV−vis spectra recorded). With an increase in the amount of silver ions, the third peak in the UV−vis spectra (Figure 8) appears and becomes gradually obvious, whereas the morphology of Au NRs was changed gradually from dumbbell to dogbone-like.

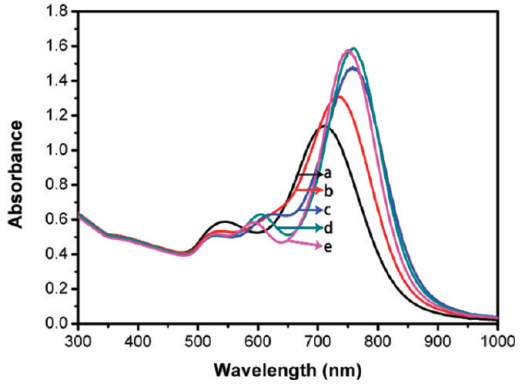

Figure 8. UV−vis spectra of resulting Au NCs produced in the presence of different concentrations of silver ions and at a fixed concentration of iodide ions (0.001 mM). The final concentrations of silver ions in the growth solution were (a) 0, (b) 0.01, (c) 0.04, (d) 0.08, and (e) 0.16 mM, respectively.

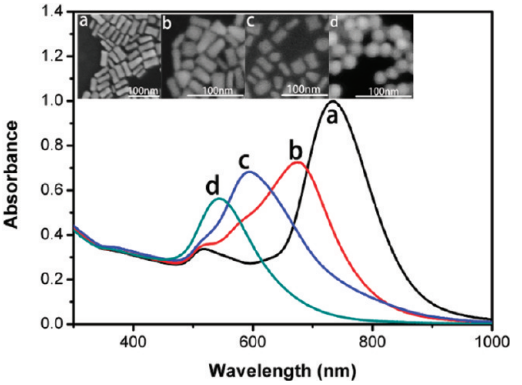

Figure 9. The UV−vis spectra of Au NCs with short aspect ratio obtained by addition of different amounts of iodide ions in the growth solution for the preparation of gold nanorods by the "seed-mediated" growth method. The final concentrations of the iodide ions in the growth solution were (a) 0.0005, (b) 0.0013, (c) 0.002, and (d) 0.02 mM, respectively. The insets are their SEM images, in which the aspect ratio of Au NRs is (a) 2.5, (b) 2, (c) 1.5, and (d) 1, respectively.

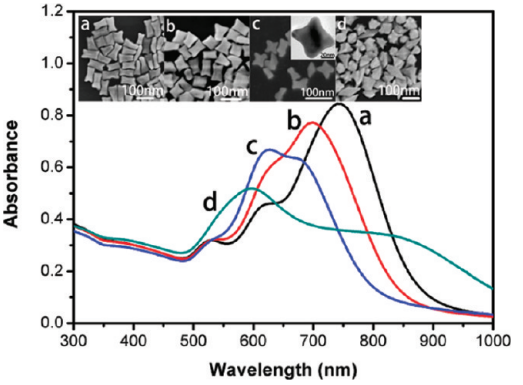

Figure 10. The UV−vis spectra of resulting Au NCs prepared in the presence of silver ions (0.06 mM) and different seeds of Au NRs with short aspect ratio from 2.5 to 1. The aspect ratio of Au NR seeds used is (a) 2.5, (b) 2, (c) 1.5 and (d) 1, respectively. The insets are their SEM images. These Au NCs with short aspect ratio seeds were obtained by addition of different amounts of iodide ions in the growth solution for preparation of gold nanorods by the "seed-mediated" growth method.

When the concentration of silver ions was 0.08 mM, the third peak was well developed. Its intensity and position was the strongest and centered at ~603 nm, (Figure 8d). In addition, the dogbone-like morphology was also well-defined. With a further increase in the amount of silver ions (0.16 mM), the third peak was still well developed (Figure 8e); however, its intensity and position became weaker and was blue-shifted to 588 nm, respectively. Accordingly, the two lobes of each tip of the dogbone-like Au crystals became obtuse gradually. When the concentration of silver ions was greater than 0.16 mM, the UV−vis spectra were unchanged.

As reported by the Liz-Marzán group, the thicker rod and well-fined dumbbell Au crystals were obtained by varying the concentration of iodide ions in the absence of silver ions. In our case, when both iodide and silver ions existed in the growth solution, the presence of silver ions in excess had no effect on the morphology change of Au NRs. Therefore, we suggest that the {111} facets at tips were mainly covered by iodide ions, not silver ions. In addition, the amount of iodide ions (0.001 mM) was only absorbed on the {111} facets on the tips, and the amount of silver ions not only was able to cover the side facets, but also can form a AgI complex with the iodide ions. Reduction of gold salt precursor on {111} facets was catalytically accelerated due to the decrease in the surface redox potential, which guarantees the formation of the dogbone-like Au crystals.

To further investigate the role of iodide and silver ions, a series of experiments were carried out. The new seeds (Figures 9 and S6) were first prepared by tuning the amounts of iodide ions in the growth solution in the "seed-mediated" growth for Au NRs. The aspect ratio of the Au NRs was decreased gradually from 2.5 to 1.5, and spherical crystal was obtained eventually. The blue shift of the LSP peak further confirmed the decrease in the aspect ratio of the Au crystals (Figure 9). All {111} facets of the new seeds were then covered by iodide ions before use. When these as-prepared seeds were separately added into the growth solution containing silver ions (0.06 mM), nanostructured Au crystals with lobes grown from {111} should be formed accordingly. As expected, dogbone-like Au crystals of short aspect ratio (Figures 10 and S7) were obtained. When the aspect ratio of the Au NRs seeds approached ~1.5, four horn-shaped cubic or cuboid Au crystals were prepared. When spherical crystals were used as seeds, spherical crystals with many thorns on them as well as bipyramids were synthesized. The diameter of the spherical part was ~40 nm, which is bigger than that of seeds with a diameter of about 26 nm. The length of the horns was in the range of 5−10 nm. It is well-known that the surface of the spherical crystals is composed of {111} and {100} facets. Therefore, the horns are grown from {111} facets,[26,44,57] whose growth was also accelerated due to the presence of iodide absorbed on them. This further confirmed that lobes were grown from the {111} facets on the tips of the Au NRs.

Accordingly, in the UV−vis spectra of as-prepared products, the intensity of the third peak caused by the lobes at the tips increases gradually and exceeds that of the LSP peak finally (Figure 10a−c) due to the decrease in the aspect ratio of the Au NR seeds. This is also because the size of the lobes is comparable to the length of as-prepared products (Tables S3 and S4). In addition, the LSP peak was also blue-shifted and has the trend to merge the third peak together.

3.6. Influence of AA on Morphology of Au NRs. The influence of ascorbic acid (AA) was also investigated under the

dx.doi.org/10.1021/jp111605j |J. Phys. Chem. C 2011, 115, 7887–7895

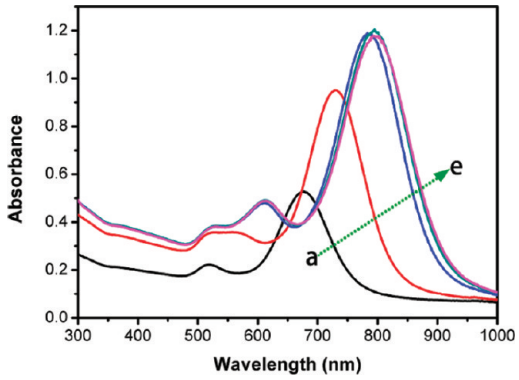

Figure 11. The UV−vis spectra of the resulting Au NCs prepared by using different amounts of AA and in the presence of silver ions (0.06 mM) and iodide ions (0.001 mM). The final concentrations of the AA in the growth solution were (a) 0.5, (b) 0.6, (c) 0.8, (d) 1.0, and (e) 1.2 mM, respectively.

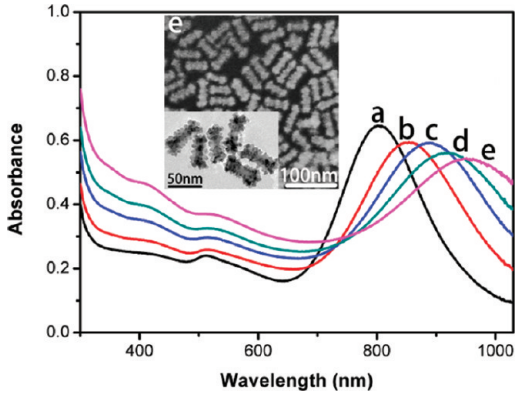

Figure 12. The UV−vis spectra of Pt-coated Au NRs produced at different concentrations of K_2PtCl_4 in the growth solution in the presence of silver ions (0.06 mM): (a) 0.05, (b) 0.125, (c) 0.2, (d) 0.275, and (e) 0.35 mM, respectively. The insets are the SEM and TEM image of sample e.

optimal conditions for formation of dogbone-like Au crystals. When the concentration of AA was lower than 0.8 mM, Au(III) could not be fully reduced to Au atoms. The remaining Au(III) in the solution would have an effect on the formed nanostructured Au crystals, which led to the formation of Au NRs with a short aspect ratio (see Figure S8).[58,59] As is expected, there is no appearance of a third peak in the UV−vis spectrum (Figure 11a). However, when the concentration of AA (>0.8 mM) was enough to reduce Au(III) to Au atoms, the same dogbone-like Au crystals formed, which was also confirmed by the UV−vis spectra (Figure 11b−e). Therefore, the role of AA in the growth of Au NRs was to reduce Au(III) rather than to affect the formation of dogbone-like Au crystals.

3.7. Color Gamut of Au NR-Based Crystals. The color gamut of a device or process is that portion of the color space that can be represented or reproduced. The color of suspensions or coatings of nanostructured Au crystals may be important in some potential applications, such as solar screening. However, only a few studies of the gamut of nanostructured Au crystals have been simulated by mapping the colors of the suspensions of the rods to the a^* and b^* color coordinates of the Commission Internationale del'Eclairage (CIE-LAB) system.[33] It was found that Au NRs display a surprisingly wide color gamut, from purple, through blue, to red, depending on their shape. Their LSP band ranges from visible close to or even in the near-IR, depending on their aspect ratio. However, there is no good way to prepare Au NRs with a high aspect ratio (>5) in high yield. To modulate their plasmon band, the controlled growth of platinum on Au NRs was conducted on the basis of previous results.

The amount of coated Pt on Au NRs can also be tuned by varying the amounts of K_2PtCl_4 at fixed concentrations of silver ions. The typical morphology of Pt NCs on Au NRs is shown in Figure 12 (the inset is the TEM image). Plenty of Pt NCs with a diameter of ∼6 nm were coated on the Au NRs. The length and width of as-prepared products are ∼60 and 25 nm, respectively. The UV−vis spectra of different Pt-coated Au NRs are shown in Figure 12. Their LSP band was maximally red-shifted to 955 nm with increasing Pt-NC-coated Au NRs. Therefore, the optical spectra of Au NR-based crystals can be tuned from visible to near-IR.

4. CONCLUSIONS

In summary, the role of silver ions, iodide ions or both as well as AA concentration during the overgrowth process of Au NRs was investigated. The growth of Au NRs can be significantly affected by silver ions alone, in which the enhanced growth of Au {111} facets results in the formation of a well-defined dogbone-like morphology. Accordingly, a third peak position at about 590 nm in the spectra of dogbone-like Au crystals appeared. In addition, the presence of small amounts of iodide in the growth solution alone results in the morphology transition of Au NRs from rods into thick rods and a dumbbell-like structure. Furthermore, the molar ratio of silver ions to iodide ions has a great effect on the final morphology of Au NRs when both are in the growth solution. The optimal concentration of silver ions and iodide ions was found to be 0.06 mM and 0.001 mM, respectively, in the formation of dogbone-like Au crystals.

The appearance of the third peak in the UV−vis spectra indicates the formation of lobes on the tips of the Au NRs. The morphology transition of Au NRs from dogbone to dumbbell can be tuned by increasing the concentration of iodide ions at fixed concentration of silver ions. However, the dogbone-like morphology of Au crystals was kept unchanged except that their lobes became obtuse when the concentration of silver ions was increased at fixed concentration of iodide ions. All mentioned results were demonstrated by TEM images and UV−vis spectra recorded.

When different seeds, such as Au NRs of short aspect ratio and spherical Au NCs, were used, horns of different length on Au seeds were formed. Taking all the results together and the cross section change in the tips of Au NRs, why two lobes instead of four were formed on each tip of the Au NRs was explained for the first time, and their growth from the {111} facets was assisted by the formation of AgI, which can catalytically reduce Au ions on those facets. Therefore, we can develop methods for the preparation of nonspherical nanostructured noble metal crystals with control over critical architectural parameters, such as the concentration of silver or halide ions during the growth process. The optical spectra of nanostructured Au crystals can be tuned from 520 to 955 nm by controlling their tip curvature or platinum coating. A wide color gamut can be readily obtained by using a random dispersion of nanostructured Au NR-based crystals.

■ ASSOCIATED CONTENT

Supporting Information. Additional information as noted in text. This material is available free of charge via the Internet at http://pubs.acs.org.

■ AUTHOR INFORMATION

Corresponding Author
*E-mails: (H. Xia) xia@icm.sdu.edu.cn. (X. Tao) txt@sdu.edu.cn.

■ ACKNOWLEDGMENT

H.X. and X.T.T. thank the Natural Science Foundation of China (Grants Nos. 50990061, 51002086, and 51021062), the 973 Program (Grant No. 2010CB630702), the Natural Science Foundation of Shandong Province (ZR2010EM006) and the Independent Innovation Foundation of Shandong University (2010JQ013) for financial support. G.W. Yu is acknowledged for AFM characterization of the Au samples.

■ REFERENCES

(1) Grzelczak, M.; Pérez-Juste, J.; Mulvaney, P.; Liz-Marzán, L. M. *Chem. Soc. Rev.* **2008**, *37*, 1783.
(2) Lu, X. M.; Rycenga, M.; Skrabalak, S. E.; Wiley, B.; Xia, Y. N. *Annu. Rev. Phys. Chem.* **2009**, *60*, 167.
(3) Xiang, Y.; Wu, X.; Liu, D.; Feng, L.; Zhang, K.; Chu, W.; Zhou, W.; Xie, S. *J. Phys. Chem. C* **2008**, *112*, 3203.
(4) Wei, W.; Li, S.; Qin, L.; Xue, C.; Millstone, J. E.; Xu, X.; Schatz, G. C.; Mirkin, C. A. *Nano Lett.* **2008**, *8*, 3446.
(5) Wiley, B.; Sun, Y.; Xia, Y. *Acc. Chem. Res.* **2007**, *40*, 1067.
(6) Murphy, C. J. *ACS Nano* **2009**, *3*, 770.
(7) Tabor, C.; Van Haute, D.; El-Sayed, M. A. *ACS Nano* **2009**, *3*, 3670.
(8) Gao, H.; Henzie, J.; Odom, T. W. *Nano Lett.* **2006**, *6*, 2104.
(9) Ni, W.; Ambjrnsson, T.; Apell, S. P.; Chen, H.; Wang, J. *Nano Lett.* **2010**, *10*, 77.
(10) Dieringer, J. A.; Wustholz, K. L.; Masiello, D. J.; Camden, J. P.; Kleinman, S. L.; Schatz, G. C.; Van Duyne, R. P. *J. Am. Chem. Soc.* **2009**, *131*, 849.
(11) Gong, X.; Yang, Y.; Huang, S. *J. Phys. Chem. C* **2010**, *114*, 18073.
(12) Nehl, C. L.; Hafner, J. H. *J. Mater. Chem.* **2008**, *18*, 2415.
(13) Khalavka, Y.; Becker, J.; Sönnichsen, C. *J. Am. Chem. Soc.* **2009**, *131*, 1871.
(14) Burgin, J.; Liu, M.; Guyot-Sionnest, P. *J. Phys. Chem. C* **2008**, *112*, 19279.
(15) Hill, H. D.; Millstone, J. E.; Banholzer, M. J.; Mirkin, C. A. *ACS Nano* **2009**, *3*, 418.
(16) Kawasaki, H.; Nishimura, K.; Arakawa, R. *J. Phys. Chem. C* **2007**, *111*, 2683.
(17) Smith, D. K.; Miller, N. R.; Korgel, B. A. *Langmuir* **2009**, *25*, 9518.
(18) Xia, H.; Bai, S.; Hartmann, J.; Wang, D. *Langmuir* **2010**, *26*, 3585.
(19) Radziuk, D.; Grigoriev, D.; Zhang, W.; Su, D.; Mohwald, H.; Shchukin, D. *J. Phys. Chem. C* **2010**, *114*, 1835.
(20) Yu, Y. Y.; Chang, S. S.; Lee, C. L.; Wang, C. R. C. *J. Phys. Chem. B* **1997**, *101*, 6661.
(21) Jana, N. R.; Gearheart, L.; Murphy, C. J. *Adv. Mater.* **2001**, *13*, 1389.
(22) Kim, F.; Song, J. H.; Yang, P. *J. Am. Chem. Soc.* **2002**, *124*, 14316.
(23) Nikoobakht, B.; El-Sayed, M. A. *Chem. Mater.* **2003**, *15*, 1957.
(24) Jana, N. R. *Small* **2005**, *1*, 875.
(25) Gou, L. F.; Murphy, C. J. *Chem. Mater.* **2005**, *17*, 3668.
(26) Sau, T. K.; Murphy, C. J. *J. Am. Chem. Soc.* **2004**, *126*, 8648.
(27) Sun, Y.; Xia, Y. *Science* **2002**, *298*, 2176.
(28) Seo, D.; Park, J. C.; Song, H. *J. Am. Chem. Soc.* **2006**, *128*, 14863.
(29) Ha, T. H.; Koo, H. J.; Chung, B. H. *J. Phys. Chem. C* **2007**, *111*, 1123.
(30) Millstone, J. E.; Park, S.; Shuford, K. L.; Qin, L.; Schatz, G. C.; Mirkin, C. A. *J. Am. Chem. Soc.* **2005**, *127*, 5312.
(31) Jeong, G. H.; Kim, M.; Lee, Y. W.; Choi, W.; Oh, W. T.; Park, Q. H.; Han, S. W. *J. Am. Chem. Soc.* **2009**, *131*, 1672.
(32) Zhang, J.; Langille, M. R.; Personick, M. L.; Zhang, K.; Li, S.; Mirkin, C. A. *J. Am. Chem. Soc.* **2010**, *132*, 14012.
(33) Xu, X.; Cortie, M. B. *Adv. Funct. Mater.* **2006**, *16*, 2170.
(34) Keul, H. A.; Möller, M.; Bockstaller, M. R. *Langmuir* **2007**, *23*, 10307.
(35) Basiruddin, S. K.; Saha, A.; Pradhan, N.; Jana, N. R. *Langmuir* **2010**, *26*, 7475.
(36) Norman, R. S.; Stone, J. W.; Gole, A.; Murphy, C. J.; Sabo-Attwood, T. L. *Nano Lett.* **2008**, *8*, 302.
(37) Leontidis, E.; Kleitou, K.; Kyprianidou-Leodidou, T.; Bekiari, V.; Lianos, P. *Langmuir* **2002**, *18*, 3659.
(38) Millstone, J. E.; Wei, W.; Jones, M. R.; Yoo, H.; Mirkin, C. A. *Nano Lett.* **2008**, *8*, 2526.
(39) Grzelczak, M.; Sánchez-Iglesias, A.; Rodríguez-González, B.; Alvarez-Puebla, R.; Pérez-Juste, J.; Liz-Marzán, L. M. *Adv. Funct. Mater.* **2008**, *18*, 3780.
(40) Magnussen, O. M. *Chem. Rev.* **2002**, *102*, 679.
(41) Rai, A.; Singh, A.; Ahmad, A.; Sastry, M. *Langmuir* **2006**, *22*, 736.
(42) Rayavarapu, R. G.; Ungureanu, C.; Krystek, P.; van Leeuwen, T. G.; Manohar, S. *Langmuir* **2010**, *26*, 5050.
(43) Song, J. H.; Kim, F.; Kim, D.; Yang, P. *Chem.—Eur. J.* **2005**, *11*, 910.
(44) (a) Liu, M.; Guyot-Sionnest, P. *J. Phys. Chem. B* **2004**, *108*, 5882. (b) Liu, M.; Guyot-Sionnest, P. *J. Phys. Chem. B* **2005**, *109*, 22192.
(45) Sau, T. K.; Murphy, C. J. *Langmuir* **2004**, *20*, 6414.
(46) Xiang, Y.; Wu, X.; Liu, D.; Jiang, X.; Chu, W.; Li, Z.; Ma, Y.; Zhou, W.; Xie, S. *Nano Lett.* **2006**, *6*, 2290.
(47) Wang, Z. L.; Mohamed, M. B.; Link, S.; El-Sayed, M. A. *Surf. Sci.* **1999**, *440*, L809.
(48) Herrero, E.; Buller, L. J.; Abruña, H. D. *Chem. Rev.* **2001**, *101*, 1897.
(49) Hubert, F.; Testard, F.; Spalla, O. *Langmuir* **2008**, *24*, 9219.
(50) Murphy, C. J.; Thompson, L. B.; Alkilany, A. M.; Sisco, P. N.; Boulos, S. P.; Sivapalan, S. T.; Yang, J.; Chernak, D. J.; Huang, J. *J. Phys. Chem. Lett.* **2010**, *1*, 2867.
(51) Sohn, K.; Kim, F.; Pradel, K. C.; Wu, J.; Peng, Y.; Zhou, F.; Huang, J. X. *ACS Nano* **2009**, *3*, 2191.
(52) Peng, X.; Manna, L.; Yang, W. D.; Wickham, J.; Scher, E.; Kadavanich, A.; Alivisatos, A. P. *Nature* **2000**, *404*, 59.
(53) Manna, L.; Scher, E. C.; Alivisatos, A. P. *J. Am. Chem. Soc.* **2000**, *122*, 12700.
(54) Peng, X. *Adv. Mater.* **2003**, *15*, 459.
(55) Peng, Z. A.; Peng, X. *J. Am. Chem. Soc.* **2001**, *123*, 1389.
(56) Sau, T. K.; Murphy, C. J. *J. Am. Chem. Soc.* **2004**, *126*, 8648.
(57) Sau, T. K.; Rogach, A. L. *Adv. Mater.* **2010**, *22*, 1781.
(58) Rodríguez-Fernández, J.; Pérez-Juste, J.; Mulvaney, P.; Liz-Marzán, L. M. *J. Phys. Chem. B* **2005**, *109*, 14257.
(59) Tsung, C. K.; Kou, X. S.; Shi, Q. H.; Zhang, J. P.; Yeung, M. H.; Wang, J. F.; Stucky, G. D. *J. Am. Chem. Soc.* **2006**, *128*, 5352.